

# Development of an Autonomous Two-Wheeled Robotic Stacker Prototype

RJ Lawrence C. Tiu and Edward B.O. Ang  
Mapúa University, Manila, Philippines  
Email: rjlawrencetiu@gmail.com, edang20@gmail.com

**Abstract**—A robotic stacker serves to lift, deliver, retrieve, and place items from one position to another. Different designs for robotic stackers have already been developed. Mobility is one characteristic of robotic stacker; this gives it the freedom to travel from one location to another. Different gripping mechanisms for the interaction with the items have also been tested by previous researchers. This research study aims to design and evaluate an autonomous two-wheeled robotic stacker prototype that will stack cylinders based on weight. The controller used for the robotic stacker is the Arduino Mega 2560. The robotic stacker uses a two-finger gripping mechanism and arm to accomplish the stacking process. For movement, a line following system was developed. Three FC-123 infrared sensors are used for the line following system. For positioning, radio-frequency identification (RFID) tags are placed on the path and serve as stopping points. A RFID reader is then attached on the robotic stacker. Three load balances weigh the three cylinders for stacking order. Stacking of the cylinders is by weight, with the heaviest cylinder at the bottom. For the results, the pose accuracy of the arm-gripper assembly was  $\pm 0.1333$  mm and  $\pm 0.2583$  mm, during no load and maximum load operation respectively. The pose repeatability of the arm-gripper assembly was  $\pm 1.2521$  mm and  $\pm 0.8112$  mm, during no load and maximum load operation respectively. After final testing, the total stack offset was 16.13 mm. Distance accuracy was found to be  $\pm 1.933$  mm, while the distance repeatability was  $\pm 10.6128$  mm. Data from the trials were not sufficient to show a correlation between the attained distances and the stack offset.

**Index Terms**—robotic stacker, line following, RFID point location system, two-finger gripper, stack alignment

## I. INTRODUCTION

In this age of technology, the number of items produced at a given time has surely increased. Advancements in production method and techniques have led to surplus in commodities. As such, storage or warehouse space is now a highly valued asset. Proper management and logistics of storage space contributes to cuts in costs. One way to address the problem of safety is to eliminate the human aspect altogether. Automation of processes has been implemented by humans to answer all the previous concerns. Automation of any process involves usage of control systems to operate machines and equipment with little to no human intervention. Studies have been

conducted on the use of automation or robots to perform the stacking process. An automated guided vehicle (AGV) has been designed by Kaloutsakis *et al.* [1]. It had a load bearing capacity of 200 kg and volume capacity of exceeding 1 m<sup>3</sup>. Aside from odometers and distance sensors, it was controlled remotely through Ethernet link. Another automated guided vehicle was designed by Wu, *et al.* as shown in Fig. 1 [2]. For use in pallet transfer, PLC was used for the motion control system. The AGV's path was guided by magnetic tapes on the floor and its location is determined by RFID. Instead of a gripper, the load-transfer mechanism used an electric push rod powered by stepper motors.



Figure 1. Material transport AGC using electric push rod [2].

An infrastructure-free AGV has been designed by Kelly, *et al.* [3]. Instead of using guidelines like magnetic tapes and color cues, the guidance system of their design involved four vision systems. The downward vision system enables the vehicle to take a mosaic of the whole space and map it accordingly. The second vision system employed a laser guidance system to determine the dimensions of the desire object to be lifted. The third is the fork hole finding vision. This vision is specifically used by the AGV to accurately determine where the forks of the lift must be situated in the pallet. Stacking vision is the last vision system. It computes the position of the initial rack to determine the height placement of the secondary rack. In order to assess robot performance, different standards have been set for the industry. The American Society for Testing and Materials (ASTM) has a committee (F45 committee) that addresses the issues of performance standards and safety with regards to

driverless automatic guided industrial vehicles. Some of the considerations are environmental effects, object detection and protection, communication and integration, and docking and navigation. ASTM F3218-17 presents standard practices for the test environment of an UAGV [4]. Some environmental factors that must be considered include lighting, temperature, ground surface, air quality, humidity and electrical interference. As such, specific test methods are prescribed given the different combinations of the varying environmental factors. Another standard is the ASTM F3244-17 [5]. This standard deals with the navigation aspect of UAGVs. These test methods evaluate the UAGV's capability to traverse a defined space. Some factors to consider are navigation system, test environment, speeds and pathing. Precision and accuracy of the UAGV in maneuvering the test environment is measured.

The International Organization for Standardization has also developed a standard for industrial robots. Termed as Manipulating Industrial Robots – Performance Criteria and Related Test Methods or ISO 9283:1998, this test method described the testing methodologies for assessing the performance characteristics of manipulating robots [6]. One study used a design of experiment method to assess the performance of the FANUC M16iL 6-axis industrial robot by Şirinterlikçi, *et al.* [7]. The data collected was only limited to a single axis. Independent variables include speed, payload, work envelope location, motion type, deceleration, and intermediate points. Also, the response variables to be measured are positional accuracy and positioning repeatability based on the ISO 9283:1998 standard. Using ANOVA to determine which factors were significant in affecting the accuracy, speed and motion type were found to be significant factors.

The main objective of this research study is to design and evaluate an autonomous two-wheeled robotic stacker prototype that can autonomously stack cylinders using Arduino code. The specific objectives that this research study aims to answer will be stated in the following statements. First specific objective is to design the Arduino controlled two-wheeled robotic stacker and its systems, namely line following system, arm-gripping assembly, and point location system using radio-frequency identification or RFID reader and tags. The second specific objective is to design the test area and the Arduino controlled load balances. The third specific objective is to evaluate the performance of the robotic stacker by measuring and calculating the following: pose accuracy, pose repeatability, distance accuracy, distance repeatability, speed test, operation time, stack alignment and stack offset, and finally, correlation between the difference in drop-off distance to stack offset.

## II. METHODOLOGICAL/CONCEPTUAL FRAMEWORK

For this research, the methodological or conceptual framework of the study is shown in Fig. 2.

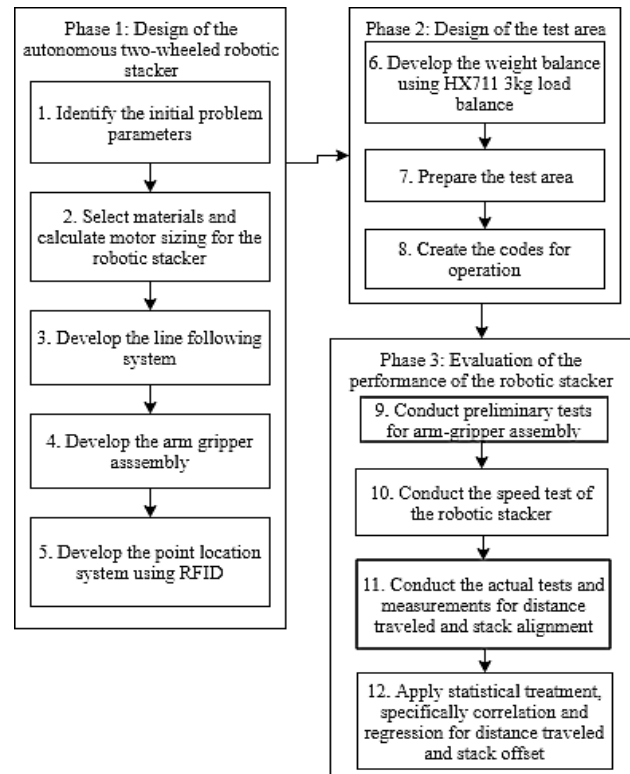


Figure 2. Methodological framework.

## III. DESIGN OF THE AUTONOMOUS MOBILE ROBOTIC STACKER

### A. Motor Sizing for the Robotic Stacker

For the robotic stacker, a stacker robot kit was used. Then, motor sizing for the stacker was computed. For wheel motor sizing, the weight of the robotic stacker was assumed to be 1 kg. For the gripper and arm, the maximum load to be carried was 0.2 kg. Also, the cylinder had a base diameter of 55 mm and a height of 60 mm. Weights for the cylinders were 77 grams, 128 grams, 178 grams. The robot kit had a two wheel and follower design. This design required two motors to run the wheels for navigation on the ground. In order to select the appropriate motor size, torque must be calculated. A derived formula for the torque of a wheel is given in equation 1.

$$T = \left(\frac{100}{e}\right) \left(\frac{(a+g \sin \theta)MR}{N}\right) \quad (1)$$

Using the initial parameters in Table I, the torque required was determined to be 0.129 kgf-cm per motor. A continuous servo is a servo that no longer has positional control, instead, it has speed control. HSR-2645CR HiTec Continuous Rotation Robot Servo was selected.

TABLE I. INITIAL PARAMETERS FOR WHEEL MOTOR SIZING

Parameter	Assumption
Total mass of the robot, $M$	1 kg
Number of drive motors, $N$	2 servo motors
Radius of the Wheels, $R$	0.0762 m

Robot Velocity, $v$	0.2 m/s
Maximum inclination, $\theta$	0 degrees
Supply Voltage, $V$	6 V
Desired acceleration, $a$	0.2 m/s <sup>2</sup>
Desired operating time	60 min
Total efficiency, $e$	60 %

Using the initial parameters in Table II, torque required for the gripper was calculated as 2.22 kgf – cm; while torque required for the arm was calculated as 9.67 kgf – cm. The selected servo for the gripper was the TowerPro MG996R Digital Servo, 11 kgf – cm torque when operating at 6V. The selected servo for the arm was the HS-785HB HiTec Winch Servo, 13.2 kgf – cm torque when operating at 6V.

TABLE II. INITIAL PARAMETERS FOR GRIPPER AND ARM MOTOR SIZING

Parameter	Assumption
Gripper finger length, $L_G$	6.5 cm
Arm length, $L_A$	20 cm
Mass of fingers, $M_F$	0.01 kg
Mass of gripper, $M_G$	0.08 kg
Mass of arms, $M_A$	0.02 kg
Mass of maximum load carried, $M_L$	0.2 kg
Motor efficiency, $e$	60%

B. Line Following System

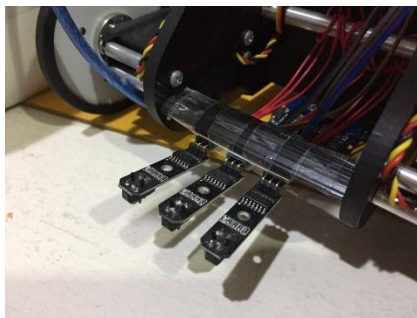


Figure 3. FC-123 line following infrared sensors.

The system uses a defined path using black electrical tape. While moving forward, the stacker should follow the path by using infrared sensors attached to the front of the robot. The path consists of black electrical tapes on a white ground surface. The black electrical tape is 20 mm in width. With this, the placement of the infrared sensors to be used must be fixed. The three infrared sensors are FC-123 line following sensors as shown in Fig. 3. The Arduino Mega 2560 will be used to power and operate the sensors. When read () command is used, the sensor will send a value from 0-1000 depending on the color reflected by the surface. Trials were done to determine the values on the two different colors to be used, namely

white and black. It was found that when the sensor is on a white surface; a value of 1000 is given. While, a value of 0 is given when the sensor is on the black electrical tape. A value of 800 is used for the line standard. With this, the left and right sensors were placed 15 mm from the center to give an allowance of 5 mm when reading the black tape.

C. Arm and Gripper Assembly

The arm and gripper system is used to pick up and drop off the cylinders. This is done using two servomotors, one to actuate the arm, and the other for the gripper. The arm moves in a vertical manner or up-down motion. The gripper movement is unidirectional along the horizontal axis or open and close motion. The cylinder weights are the following: no load (0 grams), light load (77 grams), medium load (128 grams), and heavy load (178 grams). In order to hold and release the loads, the gripper shown in Fig. 4 will have two poses. A signal of 1500 ms is designated for open, while 1200 ms is for close.

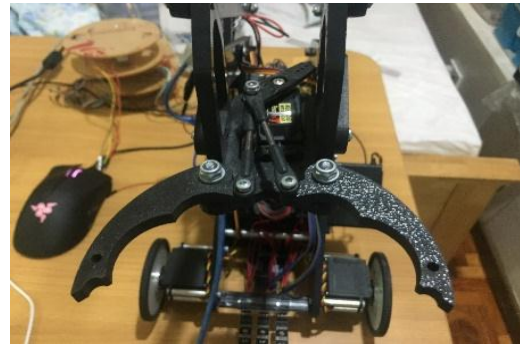


Figure 4. Two-finger gripper.

The arm will have four different poses: Pose 1 (75 mm), Pose 2 (163 mm), Pose 3 (216 mm), and Pose 4 (267 mm). To define, these poses are the heights at the tip of the gripper measured from the ground. Preliminary tests for pose positioning was conducted and discussed in chapter 6. The cycle for the testing is shown in Fig. 5. The formulas used are equation 2 and equation 3, respectively [8].

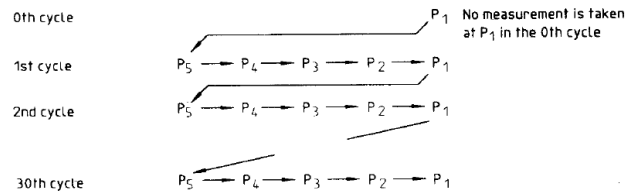


Figure 5. Cycle order for arm-gripper testing [8].

$$AP_p = \sqrt{(\bar{x} - x_c)^2 + (\bar{y} - y_c)^2 + (\bar{z} - z_c)^2} \tag{2}$$

In equation 2,  $\bar{x}, \bar{y}$  and  $\bar{z}$  are the mean coordinates of the point after repeating the same pose  $n$  times,  $x_c, y_c$  and  $z_c$  are the coordinates of the command pose, and  $x_j, y_j$  and  $z_j$  are the coordinates of the  $j$ -th attained pose [8].

$$RP_l = \bar{l} + 3S_l \tag{3}$$

$$S_l = \sqrt{\frac{\sum_{j=1}^n (l_j - \bar{l})^2}{n - 1}}$$

$$\bar{l} = \frac{1}{n} \sum_{j=1}^n l_j$$

$$l_j = \sqrt{(x_l - \bar{x})^2 + (y_l - \bar{y})^2 + (z_l - \bar{z})^2}$$

In equation 3,  $\bar{x}$ ,  $\bar{y}$  and  $\bar{z}$  are the mean coordinates of the point after repeating the same pose  $n$  times, and  $x_j$ ,  $y_j$  and  $z_j$  are the coordinates of the  $j$ -th attained pose [8].

#### D. RFID Point Location System

This section details the radio-frequency identification system or RFID system used by the robotic stacker. The purpose of this system was to determine the stopping points or stopping positions for the robotic stacker. At these points, the robotic stacker performed different operations related to pick up and drop off objects. Also, there were points that will initiate the u-turn movement of the robotic stacker. The RFID system used was Mifare MFRC522 RFID Reader/Writer. the UID of the six tags to be used in the system was determined. The RFID tags used are passive. The tags were placed on the ground along the track. The RFID reader continuously scans for tags that it may come across. Once it reads a new tag, the new UID will be compared to the code. If it matches, a certain action will be performed as written in the code. It may initiate any of the following actions: first pickup, second pickup, third pickup, first drop, second drop, third drop, or second u-turn (Table III).

TABLE III. RFID TAG AND UID

RFID Tag Name	UID in decimal
A (First Pickup)	225 143 130 53
B (Second Pickup)	225 122 120 53
C (Third Pickup)	129 25 152 53
D1 (First Drop and Second Drop)	129 145 130 53
D2 (Third Drop)	193 133 120 53
E (Second U-turn)	17 194 128 53

#### IV. DESIGN OF THE TEST AREA

This phase details the test area for the robotic stacker. The robotic stacker will move on the area and perform the operation. The area is a white illustration board 1524 mm in length and 762 mm in width. The objects placed on the area are the following: two strips of electrical tape, Arduino MEGA 2560, three HX711 3kg load balance, three cylinders shown in Fig. 6, and drop off platform.



Figure 6. Three cylinders to be stacked.

First, a second Arduino MEGA 2560 is used to control the three HX711 5kg load balance. These balances must be calibrated. The weights used to calibrate are 50 grams and 100 grams weights. TX/RX serial communication between the two Arduinos is used.

The floor of the test area is the white part of the illustration board. A red square serves as the reference point from which all other object's positions are measured. First, two straight black lines serve as the line following path for the robotic stacker. The main path contains the red square. On the line following path, a red square is placed and served as the starting point for the robotic stacker. Along the line following path, six circles labeled A, B, C, D1, D2, and E are RFID passive tags. Each of these tags has a unique identification number that will be read by the robotic stacker. Three load balances are placed in the positions described Fig. 7. The load balances are placed approximately 175 mm to 180 mm along the horizontal axis, in front of the tags. Three cylindrical weights, 55 mm in diameter, will be placed on these load balances. Lastly, a platform is used as the final drop off point. This platform is 80 mm in height and serves as the stacking point for the three cylinders. Also, this platform is located at the end of the first black path or 1033 mm from the red square.

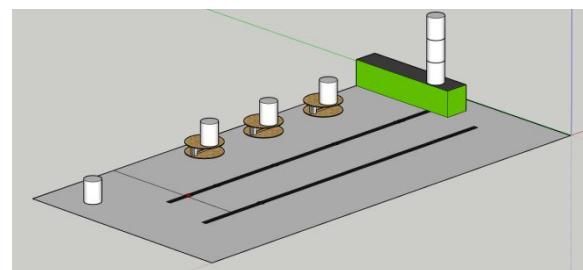


Figure 7. Isometric view of the test area.

#### V. FINAL PROGRAM AND OPERATION

To start the operation, three cylindrical weights must be placed on the three load balances. The three cylindrical weights are 77 grams, 128 grams, and 178 grams. These are then placed on the balances in six different permutations. Five trials are done for each permutation. Once the three weights are placed, the weight\_arduino will read the weights of each cylinder. The weight\_arduino will then send that information to the robotic stacker's Arduino via TX/RX serial

communication. Fig. 8 shows the wiring diagram for the Arduino-controlled robotic stacker.

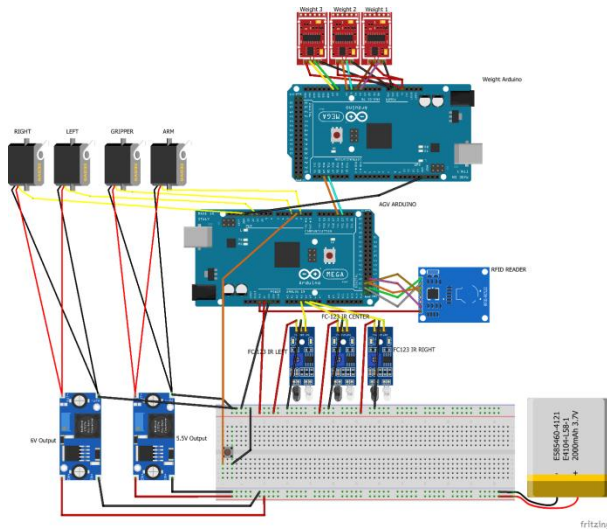


Figure 8. Wiring diagram for the robotic stacker.

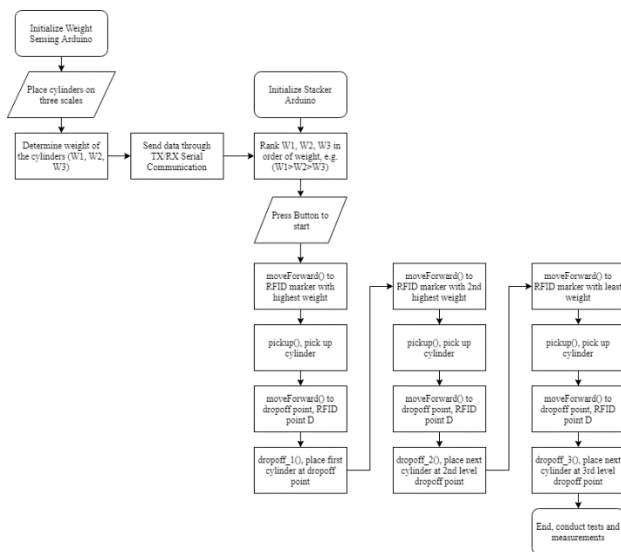


Figure 9. Programming flowchart for the stacking operation.

Next, the robotic stacker is placed on the red reference square. Serial monitor must be used to check if the robotic stacker is correctly receiving the data. Heaviest cylinder will be placed at the bottom of the stack; the lightest cylinder will be placed at the top of the stack. When the button is pressed, the robotic stacker will autonomously perform the operation. The robotic stacker will then search for the RFID tag of the heaviest weight. This may be any of the three points, A, B, or C. It will stop at this point and proceed with the pick-up process. The pick-up process consists of a 90 degree right turn, then grips the cylinder, and finally rotates back to the main black path. The arm servo will now move to the correct position of 163 mm, which is also the height for the first drop off position. It will now find the RFID tag for point D1 or the first drop off point. Once it reaches point D1, it will commence the drop off by opening the gripper. The robotic stacker will then perform a u-turn to

be on the second black path. It will then proceed to point E, where it will perform another u-turn back to the main black path. It will then search for the second heaviest and will proceed to pick it up. The arm servo will raise the cylinder to a height of 216 mm for the second drop. It will then stop at point D1 to drop off the second cylinder on top of the first cylinder. Two u-turns will be done like the previous operation. Once it is back on the main black path, the last lightest cylinder will be picked up and placed at the top of the stack. At the point D2, the last cylinder will be raised to a height of 267 mm to be placed on the stack. A programming flowchart is shown in Fig. 9.

## VI. EVALUATION OF THE ROBOTIC STACKER

### A. Pose Accuracy and Repeatability of the Arm-Gripper

Fig. 10 shows the robotic stacker in operation. Fig. 11 shows the robotic stacker prototype.



Figure 10. Robotic stacker prototype in operation.



Figure 11. Robotic stacker prototype.

Table IV details the command poses for the thirty conducted trials for no load condition. Table V details the command poses for the thirty conducted trials for maximum operating load condition. Maximum operating load is lifting a cylinder of 178 grams weight.

TABLE IV. COMMAND ANGLE AND COMMAND POSITION FOR NO LOAD CONDITION

No Load Condition		
Pose	Command Angle	Command Position
Pose 1	160	75 mm
Pose 2	110	163 mm
Pose 3	85	216 mm
Pose 4	60	267 mm

TABLE V. COMMAND ANGLE AND COMMAND POSITION FOR MAXIMUM OPERATING LOAD CONDITION

Maximum Operating Load Condition (178g)		
Pose	Command Angle	Command Position
Pose 1	160	77 mm
Pose 2	110	161 mm
Pose 3	85	214 mm
Pose 4	60	266 mm

Since the arm gripper assembly has no specifications when using the HSR-2645CRH arm servo, a target accuracy was determined. Recent advancements in accuracy standards was undertaken by an EU-funded project called COMET project. They were able to attain an accuracy of 0.05 mm for robot industry applications. For no load condition, the robot failed to attain this accuracy mark for pose 2 and pose 3 as shown in Table VI. For the maximum operating load condition, poses 2, 3, and 4 all failed the accuracy standard as shown in Table VII. These failed results may be attributed to the signal being sent or positional offshoots from the servomotor. But given the target application, which is to stack objects, the robotic stacker was able to perform the tasks commanded given the accuracies of the poses. For the pose repeatability of the assembly, there are still no specifications to compare the results. The value of the pose repeatability means that the position of the robot will be 99.8% of the time inside the repeatability range. For both conditions, pose 1 had the lowest pose repeatability. As pose 1 is the lowest position, the gripper is resting on the line following bar. For pose 2, 3, and 4, they have repeatability ranges of 1 mm to 1.5 mm.

TABLE VI. POSE ACCURACY AND POSE REPEATABILITY FOR NO LOAD CONDITION

No Load Condition					
	Pose 1 (mm)	Pose 2 (mm)	Pose 3 (mm)	Pose 4 (mm)	Average (mm)
Pose Accuracy	0.0333	0.3	0.1667	0.0333	0.1333
Pose Repeatability	0.5757	1.4824	1.4502	1.5001	1.2521

TABLE VII. POSE ACCURACY AND POSE REPEATABILITY FOR MAXIMUM OPERATING LOAD CONDITION

Maximum Operating Load Condition					
	Pose 1 (mm)	Pose 2 (mm)	Pose 3 (mm)	Pose 4 (mm)	Average (mm)
Pose Accuracy	0	0.3333	0.2667	0.4333	0.2583
Pose Repeatability	0	0.9239	1.0208	1.3001	0.8112

**B. Distance Accuracy and Repeatability of Robotic Stacker**

The attained distances of the robot were measured from the red reference point to each stop, namely A, B, C, D1, D2, and D3. The actual distance was measured along one axis, specifically from the red reference point to the bottom of the left wheel in contact with the ground. Five

trials were conducted for six permutations of pick-up operation, for a total of thirty trials. Table VIII shows the command position for each stop.

TABLE VIII. COMMAND POSITIONS FOR EACH STOP

	Stop A (mm)	Stop B (mm)	Stop C (mm)	Stop D1 (mm)	Stop D2 (mm)	Stop D3 (mm)
Command Position	195	440	700	962	962	980

Distance accuracy and distance repeatability were calculated and presented in Table IX. Stop A and Stop C both had the worst distance accuracy, close to 2 mm. But still, the robotic stacker was able to pick-up the cylinder given the inaccuracy of the stop. For the distance repeatability, Stop A had the lowest distance repeatability. This may be attributed to the short distance to be covered from the starting point to the Stop A. Also, the orientation of the robotic stacker for the start of the operation was relatively perpendicular to the line following path. The large values for the distance repeatability were mostly caused by orientation of the robotic stacker during travel. Since it is a line following robot, it might sometimes stray from the path and it would have to autonomously correct itself, thus, the orientation of the robot at the stops was not perfectly perpendicular to the path.

TABLE IX. DISTANCE ACCURACY AND DISTANCE REPEATABILITY FOR EACH STOP

	Distance Accuracy	Distance Repeatability
Stop A (mm)	2.2333	8.6279
Stop B (mm)	0.26667	11.8732
Stop C (mm)	2.3	11.2864
Stop D1 (mm)	0.4	10.9184
Stop D2 (mm)	0.2	10.8405
Stop D3 (mm)	0.2	10.1305
Average (mm)	1.9333	10.6128

**C. Stack Alignment, Stack Offset, and Stack Accuracy**

A stack is considered successful if three cylinders are stacked and do not fall. The bottom cylinder is considered the reference for the alignment of the stack. Offset 1-2 is the largest distance of the edges between the bottom cylinder and the middle cylinder. Offset 1-3 is the largest distance of the edges between the bottom cylinder and the top cylinder.

As shown in Table X, the average offset for the bottom and middle cylinder is 7.1 mm, while the average offset for the bottom and top cylinder is 9.033 mm. As observed by the researcher, the stack does not fall if the radius of the bottom of the top cylinder is still on situated on the cylinder below it. This critical radius is measured as 25 mm. As shown by the table, all trials adhered to this except trial 7. Even though the offset 1-3 of trial 7 is 29 mm, the stack did not fail because the conditions for offset 2-3 has been satisfied. Only trial 16 and trial 24 achieved a perfect stack.

TABLE X. RESULTS FOR THE ALIGNMENTS OF THE STACKS

Order of Pick-up	Trial	Offset 1-2 (mm)	Offset 1-3 (mm)	Total Offset (mm)
123	1	5	12	17
	2	18	14	32
	3	9	2	11
	4	1	7	8
	5	21	6	27
132	6	6	0	6
	7	18	29	47
	8	13	7	20
	9	0	10	10
	10	0	12	12
213	11	8	4	12
	12	13	9	22
	13	0	25	25
	14	10	8	18
	15	0	13	13
231	16	0	0	0
	17	14	10	24
	18	5	13	18
	19	12	7	19
	20	11	5	16
312	21	3	12	15
	22	17	15	32
	23	1	13	14
	24	0	0	0
	25	8	5	13
321	26	8	4	12
	27	2	2	4
	27	0	17	17
	29	7	9	16
	30	3	1	4
Average		7.1	9.03333	16.1333

Since the perfect stack should have 0 for both offsets, the stack accuracy is therefore the same as the average of the offset. Offset 1-3 has a slightly higher value than offset 1-2 because offset 1-3 is dependent on the placement of the second cylinder. The total offset is the sum of the two measured offsets.

*D. Simple Regression Analysis between Drop-off Distance and Stack Offset*

A correlational analysis was conducted between drop-off distance and stack offset. The purpose of this was to determine if the variances in drop-off distance were correlated to misalignments in the cylinder stack. A simple regression model was generated using the data found in Table XI. The first relationship to be investigated was between the difference of the attained distance of stop D1 and stop D2 vs the offset 1-2. The

difference in attained distances was the independent variable, while the offset was the dependent variable.

Minitab 17 software was used to conduct the statistical analysis. Significance level was set to 0.05. In Fig. 12, C1 was the difference between the attained distances of stop D1 and stop D2. C2 was the offset between the bottom and middle cylinder. The calculated P-value was 0.973 which was greater than the acceptable alpha level. Therefore, the relationship between the two variables were not statistically significant. Also, the correlation between the two variables was not statistically significant. The fitted line plot also verified this as the slope was 0.0059. The cause of the offsets may be due to several other factors such as orientation at the stops.

TABLE XI. DIFFERENCE IN ATTAINED DISTANCES VS OFFSET FOR FIRST AND SECOND CYLINDER

Order of Pick-up	Trial	Difference in Distances, D2 - D1 (mm)	Offset 1-2 (mm)
123	1	-14	5
	2	-5	18
	3	-12	9
	4	14	1
	5	5	21
132	6	10	6
	7	8	18
	8	12	13
	9	0	0
	10	4	0
213	11	-1	8
	12	-6	13
	13	-3	0
	14	9	10
	15	3	0
231	16	-5	0
	17	4	14
	18	2	5
	19	-2	12
	20	6	11
312	21	3	3
	22	-10	17
	23	-3	1
	24	-7	0
	25	-7	8
321	26	-3	8
	27	4	2
	28	4	0
	29	-6	7
	30	2	3
Average		0.2	7.1

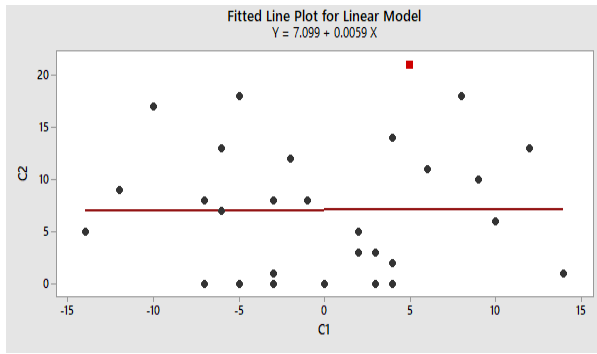


Figure 12. Fitted line plot for D2-D1 vs offset 1-2.

The second relationship to be investigated is between the differences of attained distance of stop D1 and stop D3 vs the offset 1-3 as shown in Table XII. The significance level was still set to 0.05. In Fig. 13, C3 was the difference between the attained distances of stop D1 and stop D3. C4 was the offset between the bottom and top cylinder. The initial calculated P-value was 0.098 which was still greater than the acceptable alpha level. This implies that the relationship between the two variables were not statistically significant. Also, it implies that the correlation between the two variables was not statistically significant.

TABLE XII. DIFFERENCE IN ATTAINED DISTANCES VS OFFSET FOR FIRST AND THIRD CYLINDER

Order of Pick-up	Trial	Difference in Distances, D3 – D1 (mm)	Offset 1-3 (mm)
123	1	15	12
	2	8	14
	3	18	2
	4	23	7
	5	29	6
132	6	24	0
	7	34	29
	8	26	7
	9	16	10
	10	24	12
213	11	10	4
	12	14	9
	13	0	25
	14	19	8
	15	37	13
231	16	-5	0
	17	4	10
	18	2	13
	19	-2	7
	20	6	5

312	21	17	12
	22	17	15
	23	31	13
	24	12	0
	25	14	5
321	26	19	4
	27	11	2
	27	27	17
	29	11	9
	30	17	1
Average		18.6	9.033

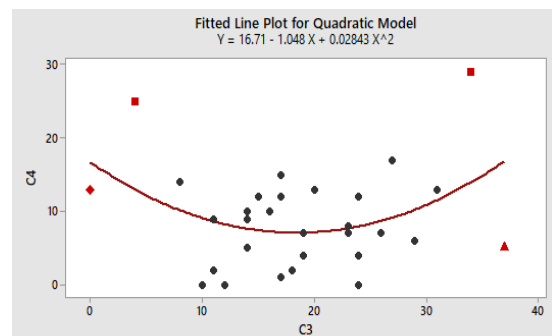


Figure 13. Fitted line plot for D3-D1 vs offset 1-3.

But the software had detected two large residual values in the plot. Upon checking, this occurred at trial 7 and trial 13. Both trials had an offset greater than or equal to 25 mm. When removing these two trials from the dataset, a new fitted line plot was generated as shown in Fig. 14. The calculated P-value was 0.969 which was greater than the acceptable alpha level. This implies that the relationship between the two variables were not statistically significant. Also, the correlation between the two variables was not statistically significant. The fitted line plot was now similar to the plot for D2-D1 vs offset 1-2.

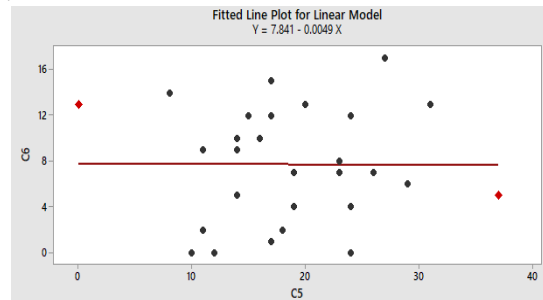


Figure 14. New fitted line plot for D3-D1 vs offset 1-3.

Again, similar issues with orientation may cause the offsets. Orientation variations may be attributed to the following reasons. First, the line following robot swerves as it corrected itself. There were some instances where the line following robot had not yet corrected itself but had already reached the drop-off point. This caused the

robotic stacker not to be oriented perfectly at the drop-off location. Second, the pose accuracy and pose repeatability of the arm gripper assembly may affect the stack. Third, the release of the gripper may affect the placement of the cylinders.

## VII. CONCLUSION

The study presents the design and evaluation of the autonomous two-wheeled robotic stacker prototype. An Arduino Mega 2560 was used as the controller of the robotic stacker. To address the problem of autonomous cylinder stacking, the robotic stacker was capable of performing the operation for thirty trials. Two sensor systems were developed to assist the robotic stacker in its operation. The first system is the line following system which consisted of three infrared sensors. As a recommendation, a five infrared sensor line following system with a proportional integral derivative controller will improve the ground movement of the robotic stacker. The second system is the point location system which used RFID reader and RFID tags. The RFID tags served as stopping points along the path. The RFID reader was used to detect the tags on the ground. A vision system may replace the RFID system for better accuracy. The arm-gripper assembly interacted with the cylinders for pick-up and drop-off operations. Two preliminary tests for pose accuracy and pose repeatability were conducted on the arm-gripper assembly, namely no load condition test and maximum operating load test. Each test consisted of four poses and the heights of each pose was measured. Results of the test show that during no load condition, the arm and gripper assembly had an average pose accuracy of  $\pm 0.1333$  mm and an average pose repeatability of  $\pm 1.2521$  mm. During maximum operating load condition, the arm and gripper assembly had an average pose accuracy of  $\pm 0.2583$  mm and an average pose repeatability of  $\pm 0.8112$  mm.

For the test area, three load balances were used to weigh the cylinders. Another Arduino Mega 2560 controlled the balances and sent the information to the robotic stacker via TX/RX serial communication. Thirty trials were conducted to evaluate the performance of the robotic stacker following ISO 9283:1998 standards. Since there are three different cylinder weights, there will be six permutations for placing on the load balances and five trials are done for each permutation. Six positions were measured for each stop, namely stop A, stop B, stop C, stop D1, stop D2, and stop D3. Average distance accuracy was found to be  $\pm 1.933$  mm, while the average distance repeatability was  $\pm 10.6128$  mm.

The cylinders were stacked according to weight, with the heaviest at the bottom and the lightest at the top. Stacked alignments of the cylinders were evaluated by measuring the stack offset. The average stack offset for the bottom and middle cylinder was 7.1 mm. For the bottom and top cylinder, it was 9.03 mm. For the average total stack offset, it was calculated to be 16.13 mm. These were considered successful stacks, since it did not surpass 50% offset criteria. Finally, correlation and regression analysis were conducted using Minitab software.

Relationship between the attained distances and the stack offset was investigated. Results showed that the relationship between the two variables was not statistically significant. Also, the correlation between the two variables was not statistically significant. The available evidence was not sufficient to conclude that the two variables correlated.

Multiple robotic stacker swarm studies may also be undertaken. Self-learning robots using artificial intelligence will enhance the capabilities and accuracy of the robotic stacker. For evaluating the robotic stacker, other factors, such as distance orientation, may be considered to determine what affects the stack alignment. Path tracking using optical cameras may be used to provide accurate and precise measurements. Other performance criteria in ISO 9283:2015 may be applied.

## CONFLICT OF INTEREST

The authors declare no conflict of interest.

## AUTHOR CONTRIBUTIONS

The main author, RJ Lawrence Tiu, conducted the research, analyzed the data, and wrote the paper. The secondary author, Edward B.O. Ang, advised the main author and introduced the main author to the scholarship program. All authors have approved the final version.

## ACKNOWLEDGMENT

The author would like to thank the Department of Science and Technology – Science Education Institute (DOST-SEI) for funding this research through its DOST-ERDT scholarship program.

## REFERENCES

- [1] G. Kaloutsakis, N. Tsourveloudis, and P. Spanoudakis, "Design and development of an automated guided vehicle," *IEEE International Conference on Industrial Technology*, vol. 2, pp. 990-993, 2003.
- [2] X. Wu, P. Lou, Q. Cai, Zhou, C. Zhou, K. Shen, and C. Jin, "Design and control of material transport system for automated guided vehicle," *UKACC International Conference on Control (CONTROL)*, pp. 765-770, 2012.
- [3] A. Kelly, B. Nagy, D. Stager, and R. Unnikrishnan, "An infrastructure-free automated guided vehicle based on computer vision," *IEEE Robotics & Automation Magazine*, pp. 24-34, 2007.
- [4] ASTM F3218-17, "Standard practice for recording Environmental effects for utilization with A-UGV test methods," *ASTM International, West Conshohocken, PA*, 2017.
- [5] ASTM F3244-17, "Standard test method for navigation: defined area," *ASTM International, West Conshohocken, PA*, 2017.
- [6] ISO 9283:1998, "Manipulating industrial robots – Performance criteria and related test methods, 1998.
- [7] A. Şirinterlikçi, M. Tiryakioğlu, A. Bird, A. Harris, K. Kweder, "Repeatability and accuracy of an industrial robot: Laboratory experience for a design of experiments course," *The Technology Interface Journal/Spring*, 2009.
- [8] ISO 9283:1998, Manipulating industrial robots – Performance criteria and related test methods, 1998.

Copyright © 2020 by the authors. This is an open access article distributed under the Creative Commons Attribution License ([CC BY-NC-ND 4.0](https://creativecommons.org/licenses/by-nc-nd/4.0/)), which permits use, distribution and reproduction in any medium, provided that the article is properly cited, the use is non-commercial and no modifications or adaptations are made.



**Tiu, RJ Lawrence C.** was born in Manila, Philippines on December 16, 1993. He earned a Bachelor of Science degree in Mechanical Engineering from Mapúa Institute of Technology, Manila, Philippines in 2015, graduating Cum Laude and Gold Medalist. He has also earned his Master of Science degree in Mechanical Engineering from Mapúa University, Manila,

Philippines in 2019. He placed 7<sup>th</sup> in the March 2015 Philippine Mechanical Engineering Board Examination. His major field of study includes mechatronics, robotics and automation.

He currently works as a part-time instructor in the School of Mechanical and Manufacturing Engineering at Mapúa University, Manila, Philippines.

Engineer Tiu is a regular member of the Philippine Society of Mechanical Engineers.